A Novel Negative Meander Line Design of Microstrip Antenna for 28 GHz mmWave Wireless Communications

Shahanawaz KAMAL [1], Abdullahi S. B. MOHAMMED [1], Mohd Fadzil BIN AIN [1], Ubaid ULLAH [2], Roslina HUSSIN [1], Zainal Arifin AHMAD [3], Mohamadariff OTHMAN [4], Mohd Fariz Ab RAHMAN [5]

[1] School of Electrical and Electronic Engineering, Universiti Sains Malaysia, Nibong Tebal 14300, Malaysia
[2] Networks and Communication Engineering Dept., Al Ain University of Science & Technology, Abu Dhabi 112612, UAE
[3] School of Materials and Mineral Resources Engineering, Universiti Sains Malaysia, Nibong Tebal 14300, Malaysia
[4] Department of Electrical Engineering, University of Malaya, Kuala Lumpur 50603, Malaysia
[5] Faculty of Bioengineering and Technology, Universiti Malaysia Kelantan - Jeli Campus, Jeli 17600, Malaysia

shahanawazkamal@gmail.com

Submitted January 13, 2020 / Accepted May 4, 2020

Abstract. *The increasing applications for nomadic computing have experienced enormous development over the preceding decade. This has eventually caused the lack of bandwidth. Therefore, to accomplish the need of consumers, compact antennas shall be designed for mmWave wireless communications. Consequently, this paper presents a novel negative meander line based microstrip antenna system being composed of inductors (L) and capacitors (C). A detailed impedance analysis of the configuration is reported. The effects of changing the radiating element's width and length on the resonant frequency have been studied. The finalized arrangement involved 243 sq. mm area and functioned at 28 GHz with a bandwidth of 2.16 GHz. At resonant frequency, the system exhibited gain and efficiency values of 8.40 dBi and 83.51%, respectively. Furthermore, the proposed design demonstrated better bandwidth and gain capabilities in comparison with the conventional microstrip patch antenna and meander line antenna.*

Keywords

Microstrip antenna, mmWave, negative meander line antenna, wireless communications

1. Introduction

The development of LTE-Advanced was predominantly driven by need for internet services [1], [2]. Still, superior capacity networks are desired to accommodate the demands of massive population. In addition, new data services and traffic types are emerging to support concepts like the e-health or smart grid. The next-generation system drivers are expected to be more diverse by supporting these applications seamlessly together with existing internet and voice services. Furthermore, the future devices are predicted to adopt new portions of spectrum where much more bandwidth is available such as the 28 GHz mmWave band.

The antenna is regarded as a critical component in any wireless communication system due to its capability to transmit or receive electromagnetic waves [3]. The most conventional version of an antenna is the microstrip arrangement, which involves a metallic patch and a ground plane printed on either side of a dielectric substrate. These printed antennas are of active interest because of their effortless manufacturing procedure, mechanical robustness and all that. However, they suffer from some limitations including large size, narrow bandwidth and low gain. Research clarifies that wide antenna bandwidth can be accomplished by employing several techniques for instance, optimizing impedance matching [4], mounting parasitic elements [5], incorporating thick substrates [6], integrating multiple resonances [7], exercising low effective permittivity substrate [8], and employing reactive impedance surface [9]. However, these methods experience a few notable complexities like spurious coupling, larger extent, reduced efficiency and low gain.

Recently, scholars have presented several printed antenna design procedures for mmWave wireless communications. Thomas et al. [2] demonstrated a method of combining rectangular and circular patch to achieve a gain of 6.62 dBi only. Similarly, Jandi et al. [10] utilized a rectangular patch. In this antenna system however with compact dimension, the resultant bandwidth and efficiency did not appear to be optimum. In another approach, Yoon and Seo [11] exercised multiple slots in the radiating patch but found that a bandwidth of 3.35 GHz and a gain of 13 dBi can be achieved at the cost of increased board area.

Generally, the conductors in a meander line approach are fashioned by a sequence of sets of right-angled bends to obtain configuration simplicity, large bandwidth and to reduce the radiating element's overall size [12–17]. However, this arrangement suffers from poor radiation efficiency [18]. An efficient solution to overcome this shortcoming and enhance the transmission magnitude is to etch periodic slots on the metal plate [19]. Therefore, this paper presents a novel miniature design of radiating elements

Reference No.	Area (mm^2)	Size (λ_0^2)	Bandwidth (GHz)	Gain (dBi)	Efficiency (%)
[10]	361.00	1.77 × 1.77	1.00	8.03	58.00
[11]	1899.80	3.85 × 4.29	3.35	13.00	N.A.
[20]	196.00	1.32 × 1.32	2.66	5.40	93.00
[21]	576.00	2.24 × 2.24	1.70	15.20	84.00
[22]	420.00	1.96 × 1.86	6.00	7.00	N.A.
[23]	217.00	0.56 × 0.56	1.20	13.50	99.30
[24]	597.00	1.85 × 2.80	1.50	7.41	N.A.
[25]	400.00	1.86 × 1.86	0.85	8.00	N.A.
[26]	1050.00	2.80 × 3.26	4.10	8.30	82.00
[27]	1113.00	5.00 × 2.00	3.32	10.6	91.00
[28]	1219.00	4.94 × 2.14	1.90	9.26	94.00
Proposed	243.00	2.52 × 0.84	2.16	8.40	83.51

Tab. 1. Comparison of antenna designs at 28 GHz.

called as a negative meander line antenna for mmWave applications. The proposed configuration incorporated meander line shaped slots between the microstrip line patches to function like a combination of capacitors and inductors. The finalized arrangement occupied 27 × 9 mm² of board area to operate with a bandwidth of 2.16 GHz and a gain of 8.40 dBi. Table 1 reviews the particulars of a few antenna designs for the 28 GHz millimeter wave band.

2. The Negative Meander Line Antenna

2.1 Design and Impedance Analysis

The geometry of negative meander line antenna system is shown in Fig. 1(a) and 1(b). CST Microwave Studio software [29] has been utilized for simulation purposes. Taking into account the two adjacent unit cells illustrated in Fig. 1(c), the two microstrip line patches will be at potentials $\pm V$ contributing to an increase in the gap capacitance (C). The current flow through the microstrip line assembly acts as an inductor with inductance (L). The equivalent circuit of the adjacent microstrip line patches can be indicated as specified in Fig. 1(d). Duroid RO4003C microwave substrate with a thickness of 0.813 mm and dielectric permittivity of 3.38 was utilized to construct the system as depicted in Fig. 1(e). Their design parameters are tabulated in Tab. 2. A 2.4 mm series blunt post connector, model no. HPC4312-12, manufactured by A-Info Inc was used for the antenna prototype.

The value of capacitance can be determined with the help of Fig. 1(c) where, a line $z = 0$ is assumed at the middle i.e. between the microstrip line structures. Considering the 1 mm distance d between microstrip line patches, the gap capacitance per unit length can be estimated from the subsequent equation [30], [31],

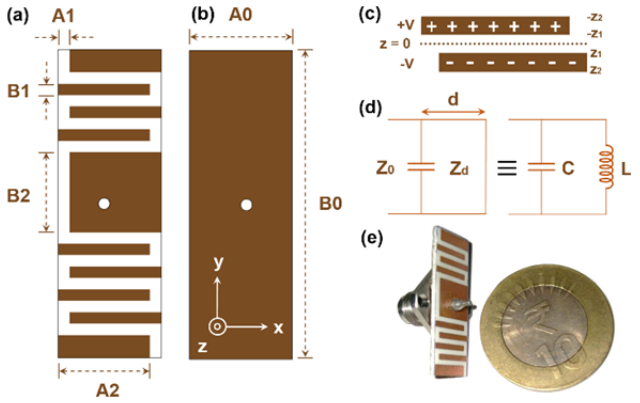

Fig. 1. (a) Top view and (b) bottom view of the proposed negative meander line configuration; (c) coplanar adjacent microstrip line patches at potentials ±V giving rise to a gap capacitance; (d) its equivalent circuit and (e) the fabricated antenna.

Parameter	A0	A1	A2	B0	B1	B2
Value (mm)	9	1	8	27	1	7

Tab. 2. Parameter values.

$$C_0 = \frac{\varepsilon K(k')}{K(k)} \tag{1}$$

where $k = z_1/z_2$, $k' = \sqrt{1-k^2}$ and z_1, z_2 are the z-coordinates of the edges of the microstrip line as depicted in Fig. 1 (c). The complete elliptical integral can be articulated from the next calculation [31],

$$K(z) = \int_0^{\pi/2} \frac{\mathrm{d}\phi}{\sqrt{(1 - z^2 \sin^2 \phi)}} = \frac{\pi}{2}\left(1 + \frac{1^2}{2^2} z^2 + \frac{1^2 3^2}{2^2 4^2} z^4 + \frac{1^2 3^2 5^2}{2^2 4^2 6^2} z^6 + \ldots\right), \quad z^2 < 1. \tag{2}$$

After neglecting the higher order terms of $K(z)$, the above equation can be written as,

$$K(z) \approx \frac{\pi}{2}\left(1 + \frac{1^2}{2^2} z^2\right). \tag{3}$$

Considering the length of every single microstrip line to be s with half of the electric field in air and the remaining field in the dielectric substrate [31], the total capacitance can be obtained using the following expression,

$$C \approx C_0 s\,. \tag{4}$$

The surface impedance $\eta = \mathrm{j}v$ from the equivalent circuit representation in Fig. 1(d) can be plotted by using the successive equations [31],

$$\eta = Z_{\mathrm{LC}} = \mathrm{j}\frac{X_{\mathrm{L}} X_{\mathrm{C}}}{X_{\mathrm{C}} - X_{\mathrm{L}}} = \mathrm{j}X_{\mathrm{LC}} \tag{5}$$

where

$$X_{\mathrm{L}} = Z_{\mathrm{d}} \tan(kd)\,, \tag{6}$$

$$k = k_0 \sqrt{\varepsilon_{\mathrm{r}}}\,, \tag{7}$$

$$Z_{\mathrm{d}} = \frac{\eta_0}{\sqrt{\varepsilon_{\mathrm{r}}}}, \quad X_{\mathrm{c}} = \frac{1}{\omega C}. \qquad (8), (9)$$

2.2 Magnitude of S11

The operating principle of negative meander line antenna system was studied by concentrating on four categories (A, B, C and D) that we have defined. For a Category-A Antenna, the overall dimension of the system was decided by varying the number N of capacitive fingers from one to nine (Fig. 2). Here, the width (A2) and length (B2) of the inductive finger were kept stable at 8 mm and 7 mm, respectively. The desired result of 28 GHz operating frequency was yielded when nine capacitive fingers along with one inductive finger were employed. A rise in the total inductance was observed with an increase in the wire's length. Even though adding fingers witnessed a decrease in the overall capacitance.

For a Category-B Antenna, the total size (27 × 9 mm²) of the system was kept constant, while the width (A2) of capacitive or inductive fingers was allowed to vary. Nine distinct sizes from 1 mm to 9 mm were considered (Fig. 3). An optimum outcome was observed for A2 = 8 mm.

For a Category-C Antenna, the length (B1) and width (A2) of capacitive fingers were fixed to 1 mm and 8 mm, respectively. Also, the width (A2) of inductive finger was set to 8 mm. However, the length (B2) of the inductive finger was varied from 1 mm to 9 mm (Fig. 4). It is evident from the magnitude of S11 curves that B2 = 7 mm is ideal for 28 GHz resonance.

For a Category-D Antenna, the absolute extent of system was set to 243 mm^2. However, parametric simulation analyses were performed for deciding the length (B1) of capacitive fingers. Four unique cases were examined notably 0.5 mm, 1.0 mm, 1.5 mm and 2.0 mm (Fig. 5). The arrangement with B1 = 1.0 mm showed magnitude of S11 value of –23.866 dB at 28 GHz and covered the frequencies of 27.039 GHz to 29.199 GHz.

Briefly, a comparable effect on the overall capacitance was observed for all the categories of antenna. The results illustrated in Figs. 2 to 5 prove that the anticipated

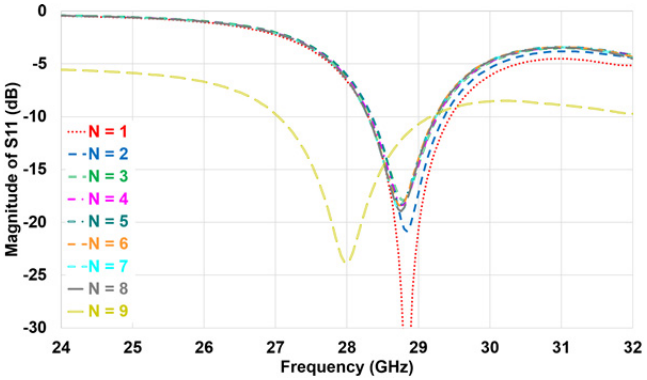

Fig. 2. Simulated magnitude of S11 with variation in the number N of capacitive fingers of the proposed negative meander line antenna.

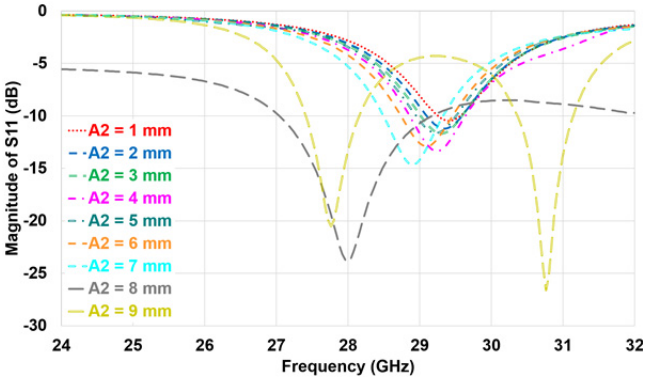

Fig. 3. Simulated magnitude of S11 with variation in the width (A2) of capacitive or inductive fingers of the proposed negative meander line antenna.

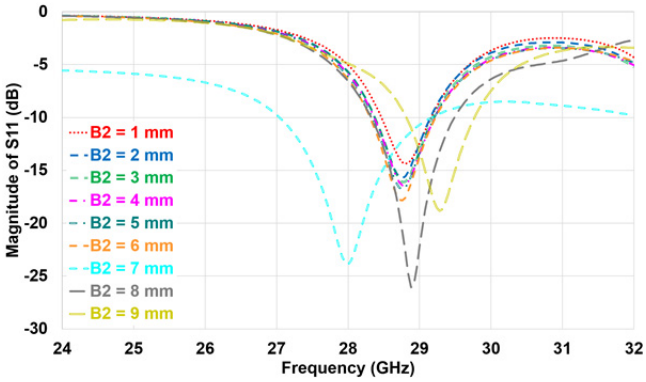

Fig. 4. Simulated magnitude of S11 with variation in the length (B2) of inductive finger of the proposed negative meander line antenna.

resonance of 28 GHz could be achieved with the parameter values mentioned in Tab. 1. Furthermore, an ideal position of the coaxial feed was determined by studying nine different locations (L) as shown in Fig. 6. These include (*x*, *y*) mm = (4, 13), (4, 13.5), (4, 14), (4.5, 13), (4.5, 13.5), (4.5, 14), (5, 13), (5, 13.5), and (5, 14). The finest results were accomplished for (4, 13.5) mm. Consequently, an antenna was constructed by employing these optimum dimensions. Their measurements were performed by utilizing Agilent's N5245A PNA-X Microwave Network Analyzer (Fig. 6).

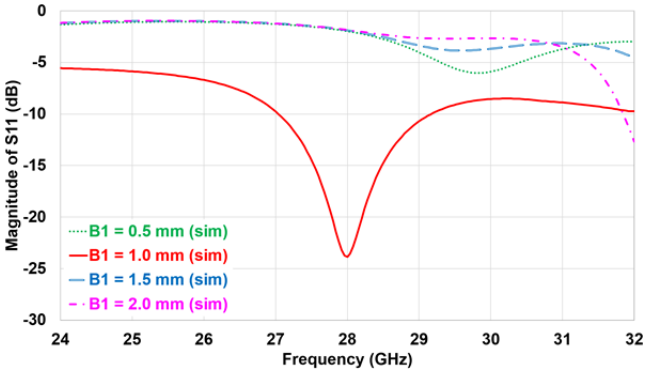

Fig. 5. Simulated magnitude of S11 with variation in the length (B1) of capacitive fingers and measured magnitude of S11 of the proposed negative meander line antenna.

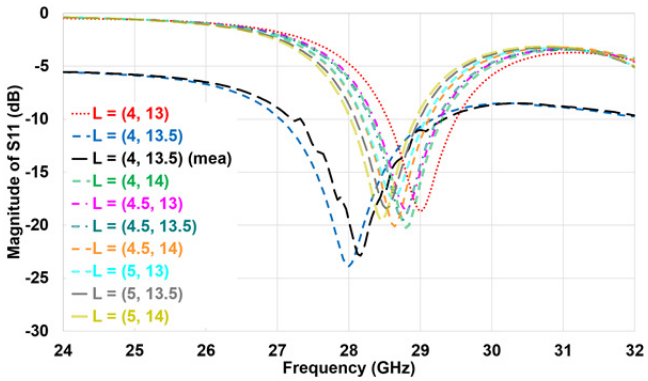

Fig. 6. Simulated magnitude of S11 with variation in locations (L) of the coaxial feed of the proposed negative meander line antenna.

2.3 E-Field Vector and Surface Current Distributions

The simulated e-field vector and surface current distributions of the concluded configuration at 28 GHz are shown in Fig. 7(a) and 7(b), respectively. A coaxial feed probe was employed to excite the system and yield the charge distributions. This converted the TEM mode into the parallel plate mode across the probe aperture and thereby confined the higher-order mode's evanescent waves. Furthermore, the zero-order mode propagated away to excite the antenna's TM10 resonant mode. A charge density was witnessed around the edges due to the repulsive force between these positive charges. In this way, the fringing fields produced by the charges led to radiation. Briefly, the vital electric fields were produced from the capacitive fingers whereas the ground plane participated in suppressing the back radiation which ultimately improved the impedance matching of the radiating element.

2.4 Radiation Pattern

Figure 8 shows the simulated and measured radiation patterns of the proposed negative meander line antenna in

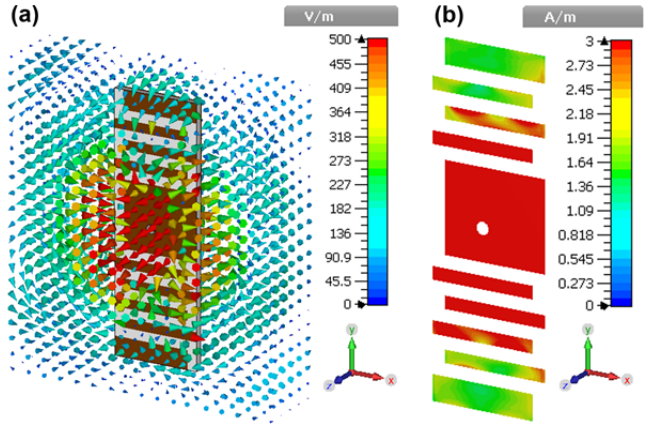

Fig. 7. Simulated (a) e-field vector and (b) surface current distributions of the proposed negative meander line antenna at 28 GHz.

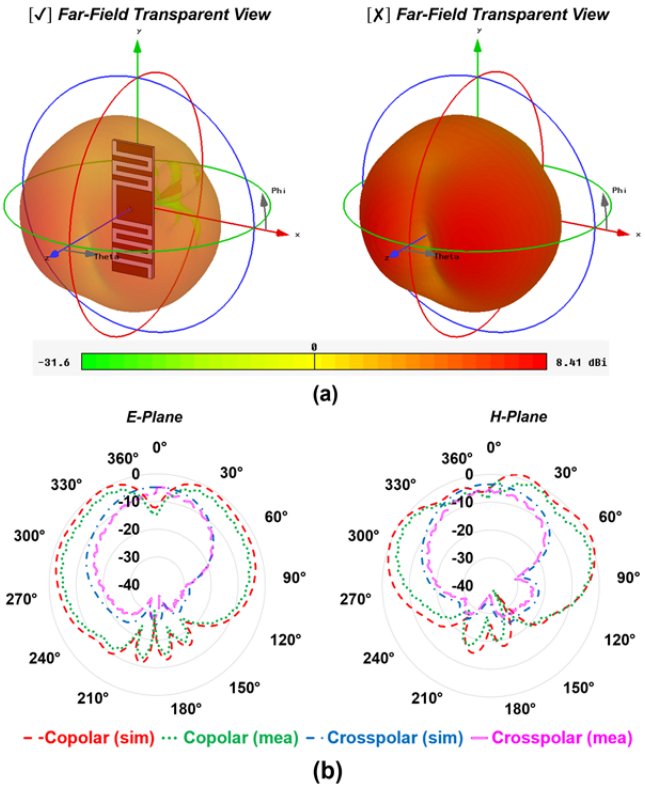

Fig. 8. (a) Simulated 3D radiation patterns of the proposed negative meander line antenna at 28 GHz. (b) Simulated and measured 2D radiation patterns of the proposed negative meander line antenna at 28 GHz.

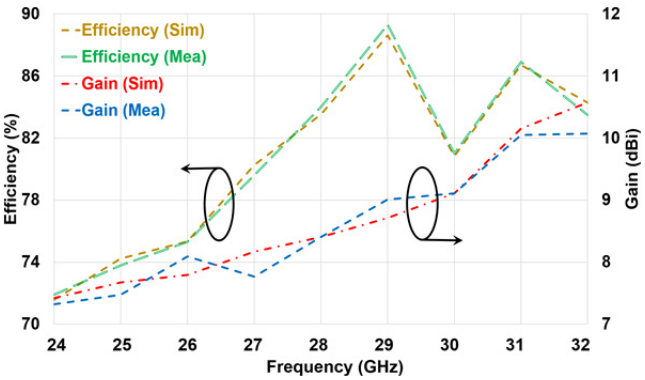

Fig. 9. Efficiency and gain of the proposed negative meander line antenna.

two planes namely, E and H planes for operating frequency at 28 GHz. The E and H planes patterns were computed practically at the Anechoic Chamber, Universiti Sains Malaysia. In the proposed negative meandering technique, there is no physical connection between the patch at the center and the adjacent metallic strips. Therefore, the patch acts as the main radiator and the adjacent disconnected microstrip lines act as parasitic elements which eventually add up the antenna gain in phase. Moreover, the radiation patterns were approximately omnidirectional. At 28 GHz resonant frequency, the proposed negative meander line antenna displayed gain and efficiency values of 8.40 dBi and 83.51%, respectively, Fig. 9.

3. Performance Comparison of the Proposed Design with the Conventional Antenna Systems

Generally, meander line antennas are designed by bending the arms of a microstrip dipole at right angles to establish an electrically larger radiating element in a smaller area [12], [13]. In order to evaluate the performance of the proposed negative meander line antenna, a conventional microstrip patch antenna and a meander line antenna was designed using CST Microwave Studio software [19]. The typical configuration of a meander line antenna, described in Fig. 10(a) and Tab. 2, was obtained by replacing the microstrip line patches of the proposed antenna with slots and vice versa. Additionally, a conventional microstrip patch antenna, illustrated in Fig. 10(c), was designed by employing equations mention in [32–34]. Duroid RO4003C with a thickness of 0.813 mm and dielectric permittivity of 3.38 was utilized as the substrate. It is evident from the results shown in Fig. 10 that the meander line antenna and the microstrip patch antenna offer a bandwidth of 1.24 GHz and 1.16 GHz, respectively, which is very less as compared to the proposed design. Similarly, the negative meander line antenna system demonstrated a comparatively better gain of 8.40 dBi with a reasonable efficiency of 83.51%. The results of all the three configurations are summarized in Tab. 3.

Antenna Configuration	Size (λ_0^2)	Bandwidth (GHz)	Gain (dBi)	Efficiency (%)
Microstrip Patch	1.17 × 1.35	1.16	4.58	85.59
Meander Line	2.52 × 0.84	1.24	6.90	47.99
Negative Meander Line	2.52 × 0.84	2.16	8.40	83.51

Tab. 3. Performance comparison of the conventional microstrip patch antenna, meander line antenna and the proposed negative meander line antenna at 28 GHz.

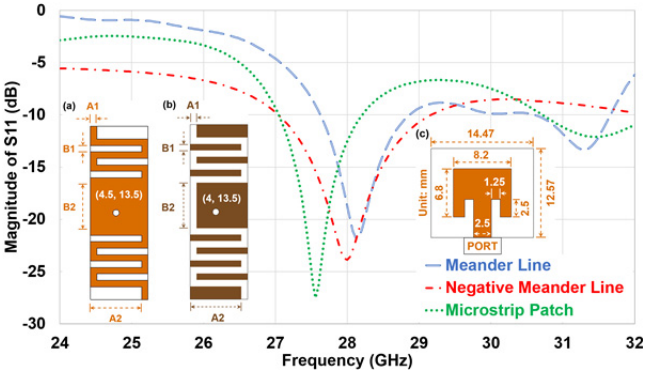

Fig. 10. Simulated magnitude of S11 curves with top views of (a) meander line antenna, (b) negative meander line antenna and (c) microstrip patch antenna.

4. Conclusion

In this paper, a novel negative meander line antenna was presented to be used in the 28 GHz mmWave frequency band. The system occupied 27 × 9 mm^2 of board area and overall height of 0.813 mm. The manufactured antenna was tested in a laboratory which demonstrated an accurate simulation and measurement outcomes agreement. The results confirmed a superior bandwidth and gain values compared with the conventional microstrip patch antenna and the meander line antenna. In addition, the proposed system involved a simple layout which ultimately confirms an appreciable choice for incorporation with the recent compact devices.

Acknowledgment

This work was supported by the Ministry of Higher Education, Malaysia under Fundamental Research Grant Scheme 203.PELECT.6071429.

References

[1] OSSEIRAN, A., MONSERRAT, J. F., MARSCH, P. *5G Mobile and Wireless Communications Technology*. Cambridge University Press, 2016. DOI: 10.1017/cbo9781316417744

[2] THOMAS, T., VEERASWAMY, K., CHARISHMA, G. Mm wave MIMO antenna system for UE of 5G mobile communication: Design. In *2015 Annual IEEE India Conference (INDICON)*. New Delhi (India), 2015, p. 1–5. DOI: 10.1109/indicon.2015.7443471

[3] BALANIS, C. A. *Antenna Theory: Analysis and Design*. 4th ed. John Wiley & sons, 2016. ISBN: 978-1-118-64206-1

[4] CHAUHAN, B., VIJAY, S., GUPTA, C. S. Millimeter-wave mobile communications microstrip antenna for 5G-A future antenna. *International Journal of Computer Applications,* 2014, vol. 99, no. 19, p. 15–18. DOI: 10.5120/17481-8303

[5] MATIN, M. A., SHARIF, B. S., TSIMENIDIS, C. C. Dual layer stacked rectangular microstrip patch antenna for ultra wideband applications. *IET Microwaves, Antennas & Propagation,* 2007, vol. 1, no. 6, p. 1192–1196. DOI: 10.1049/iet-map:20070051

[6] CHATTOPADHYAY, S. (ed.) *Trends in Research on Microstrip Antennas*. IntechOpen, 2017. DOI: 10.5772/65580

[7] LIU, N.-W., ZHU, L., CHOI, W.-W., et al. A low-profile aperture-coupled microstrip antenna with enhanced bandwidth under dual resonance. *IEEE Transactions on Antennas and Propagation,* 2017, vol. 65, no. 3, p. 1055–1062. DOI: 10.1109/tap.2017.2657486

[8] SAED, M. A., YADLA, R. Microstrip-fed low profile and compact dielectric resonator antennas. *Progress In Electromagnetics Research,* 2006, vol. 56, p. 151–162. DOI: 10.2528/pier05041401

[9] KAMAL, S., CHAUDHARI, A. A. Printed meander line MIMO antenna integrated with air gap, DGS and RIS: A low mutual coupling design for LTE applications. *Progress In Electromagnetics Research C,* 2017, vol. 71, p. 149–159. DOI: 10.2528/pierc16112008

[10] JANDI, Y., GHARNATI, F., SAID, A. O. Design of a compact dual bands patch antenna for 5G applications. In *2017 International Conference on Wireless Technologies, Embedded and Intelligent Systems (WITS)*. Fez (Morocco), 2017, p. 1–4. DOI: 10.1109/wits.2017.7934628

[11] YOON N., SEO, C. A 28-GHz wideband 2 × 2 U-slot patch array antenna. *Journal of Electromagnetic Engineering and Science,* 2017, vol. 17, no. 3, p. 133–137. DOI: 10.5515/jkiees.2017.17.3.133

[12] CALLA, O. P. N., SINGH, A., SINGH, A. K., et al. Empirical relation for designing the meander line antenna. In *2008 International Conference on Recent Advances in Microwave Theory and Applications.* Jaipur (India), 2008, p. 695–697. DOI: 10.1109/amta.2008.4762995

[13] TAKAHASHI, T., HIRASAWA, K. A broadband rectangular-cavity-backed meandering slot antenna. In *IEEE International Workshop on Antenna Technology: Small Antennas and Novel Metamaterials (IWAT 2005)*. Singapore, 2005, p. 21–24. DOI: 10.1109/iwat.2005.1460986

[14] GUPTA, A. K., KUMAR, N. Dual band meander slot antenna for mobile applications. In *2015 International Conference on Communications and Signal Processing (ICCSP).* Melmaruvathur (India), 2015, p. 0828–0830. DOI: 10.1109/iccsp.2015.7322609

[15] BODDU, V. S., CHILUKURI, S. A multi band planar inverted-F antenna with meandered slots for mobile applications. In *2019 IEEE-APS Topical Conference on Antennas and Propagation in Wireless Communications (APWC).* Granada (Spain), 2019, p. 431–435. DOI: 10.1109/apwc.2019.8870466

[16] SUKHIJA, S., SARIN, R. K. A U-shaped meandered slot antenna for biomedical applications. *Progress In Electromagnetics Research M,* 2017, vol. 62, p. 65–77. DOI: 10.2528/pierm17082101

[17] ALLEN, C. M., ELDEK, A. A., ELSHERBENI, A. Z., et al. Dual tapered meander slot antenna for radar applications. *IEEE Transactions on Antennas and Propagation,* 2005, vol. 53, no. 7, p. 2324–2328. DOI: 10.1109/tap.2005.850757

[18] BALANIS, C. B. *Antenna Theory: Analysis and Design.* 3rd ed. John Wiley, 2005. (Ch. 14, Microstrip antennas.) ISBN: 978-0471667827

[19] PUSHPAKARAN, S. V., PURUSHOTHAMAN, J. M., CHANDROTH, A., et al. An extraordinary transmission analogue for enhancing microwave antenna performance. *AIP Advances,* 2015, vol. 5, no. 10, p. 1–5. DOI: 10.1063/1.4935193

[20] RAHMAN, A., YI, N. M., AHMED, A. U., et al. A compact 5G antenna printed on manganese zinc ferrite substrate material. *IEICE Electronics Express,* 2016, vol. 13, no. 11, p. 1–5. DOI: 10.1587/elex.13.20160377

[21] KHALILY, M., TAFAZOLLI, R., RAHMAN, T., et al. Design of phased arrays of series-fed patch antennas with reduced number of the controllers for 28-GHz mm-wave applications. *IEEE Antennas and Wireless Propagation Letters,* 2015, vol. 15, p. 1305–1308. DOI: 10.1109/lawp.2015.2505781

[22] KARTHIKEYA, G. S., ABEGAONKAR, M. P., KOUL, S. K. CPW fed conformal folded dipole with pattern diversity for 5G mobile terminals. *Progress In Electromagnetics Research C,* 2018, vol. 87, p. 199–212. DOI: 10.2528/pierc18082902

[23] KHATTAK, M. I., SOHAIL, A., KHAN, U., et al. Elliptical slot circular patch antenna array with dual band behaviour for future 5G mobile communication networks. *Progress In Electromagnetics Research C,* 2019, vol. 89, p. 133–147. DOI: 10.2528/pierc18101401

[24] PARK, J. S., KO, J. B., KWON, H. K., et al. A tilted combined beam antenna for 5G communications using a 28-GHz band. *IEEE Antennas and Wireless Propagation Letters,* 2016, vol. 15, p. 1685–1688. DOI: 10.1109/LAWP.2016.2523514

[25] ZHANG, Y., DENG, J., LI, M., et al. A MIMO dielectric resonator antenna with improved isolation for 5G mm-wave applications. *IEEE Antennas and Wireless Propagation Letters,* 2019, vol. 18, p. 747–751. DOI: 10.1109/LAWP.2019.2901961

[26] KHALID, M., NAQVI, S. I., HUSSAIN, N., et al. 4-port MIMO antenna with defected ground structure for 5G millimeter wave applications. *Electronics,* 2020, vol. 9, no. 1, p. 1–13. DOI: 10.3390/electronics9010071

[27] KAMAL, S., MOHAMMED, A. S. B., AIN, M. F., et al. A novel lumped LC resonator antenna with air-substrate for 5G mobile terminals. *Progress In Electromagnetics Research Letters,* 2020, vol. 88, p. 75–81. DOI: 10.2528/PIERL19090509

[28] KAMAL, S., MOHAMMED, A. S. B., AIN, M. F., et al. 28 GHz mm-wave quasi-lumped element resonator antenna on air-substrate. In *2019 IEEE Asia-Pacific Conference on Applied Electromagnetics (APACE).* Melacca (Malaysia), 2019, p. 1–4. DOI: 10.1109/APACE47377.2019.9020741

[29] CST MICROWAVE STUDIO, LLC, US: Computer Simulation Technology Studio Suite.

[30] HONG, J.-S. G., LANCASTER, M. J. *Microstrip Filters for RF/Microwave Applications.* John Wiley & Sons, 2004. ISBN: 978-0-471-46420-4

[31] MOSALLAEI, H., SARABANDI, K. Antenna miniaturization and bandwidth enhancement using a reactive impedance substrate. *IEEE Transactions on Antennas and Propagation,* 2004, vol. 52, no. 9, p. 2403–2414. DOI: 10.1109/tap.2004.834135

[32] JAMES, J. R., HALL, P. S. (Eds.) *Handbook of Microstrip Antenna,* London (UK): IET, 1989. ISBN: 9780863411502

[33] KARA, M. Closed-form expressions for the resonant frequency of rectangular microstrip antenna elements with thick substrates. *Microwave and Optical Technology Letters,* 1996, vol. 12, no. 3, p. 131–136. DOI: 10.1002/(SICI)1098-2760(19960620)12:3<131::AID-MOP4>3.0.CO;2-I

[34] DERNERYD, A. G. A theoretical investigation of the rectangular microstrip antenna element. *IEEE Transactions on Antennas and Propagation,* 1978, vol. 26, no. 4, p. 532–535. DOI: 10.1109/TAP.1978.1141890

About the Authors ...

Shahanawaz KAMAL (corresponding author) was born in Mumbai, India. He received the B.E. and M.E. degrees in Electronics and Telecommunication Engineering from the University of Mumbai, India in 2013 and 2017, respectively. He is currently working toward the Ph.D. degree in Antenna and Propagation with the School of Electrical and Electronic Engineering, Universiti Sains Malaysia, Malaysia. He joined Vedang Cellular Services Pvt. Ltd., India as an In-Building Solution (IBS) Engineer in 2014. He was a Visiting Lecturer at the Department of Information Technology, M. H. Saboo Siddik Polytechnic, India in 2016. His research interests include conceptualization, design, development and measurement of PCB or sheet metal antennas with single element, array and MIMO configurations for ISM, LTE, mmWave and 5G applications.

Abdullahi S. B. MOHAMMED received the B.Eng. degree in Electrical Engineering from Bayero University Kano, Nigeria in 2008, and the M.Sc. degree in Electrical Engineering with prime focus on telecommunication from Ahmadu Bello University, Nigeria in 2014. He is currently working toward the Ph.D. degree in antenna and propagation with the School of Electrical and Electronic Engineering, Universiti Sains Malaysia, Malaysia.

Mohd Fadzil BIN AIN received the B.S. degree in Electronic Engineering from Universiti Teknologi Malaysia, Malaysia in 1997; the M.S. degree in Radio Frequency and Microwave from Universiti Sains Malaysia (USM), Malaysia in 1999; and the Ph.D. degree in Radio Frequency and Microwave from the University of Birmingham, United Kingdom in 2003. In 2003, he joined the School of Electrical and Electronic Engineering, USM. He is currently a Professor with VK7 grade, the Dean of Research, Postgraduate and Networking, and the Director of Collaborative Microelectronic Design Excellence Centre (CEDEC). He is actively involved in technical consultancy with several companies in repairing microwave equipment. His current research interests include MIMO wireless system on FPGA/DSP, Ka-band transceiver design, dielectric antenna, RF characterization of dielectric material, and microwave propagation study. Dr. Ain's awards and honors include International Invention Innovation Industrial Design and Technology Exhibition, International Exposition of Research and Inventions of Institutions of Higher Leaning, Malaysia Technology Expo, Malaysian Association of Research Scientists, Seoul International Invention Fair, iENA, Best Paper for the 7th WSEAS International Conference on Data Networks, Communications, Computers, and International Conference on X-Ray & Related Techniques in Research and Industry.

Ubaid ULLAH received the M.S. and Ph.D. degrees in Electronic Engineering from Universiti Sains Malaysia, Malaysia in 2012 and 2017, respectively. He was a Post-Doctoral Researcher at the School of Science and Engineering, Reykjavik University, Iceland. He has published several articles in ISI indexed journals and some well-reputed international conferences. His current research interests include dielectric resonator antennas (DRAs), wideband DRAs, microwave circuits, low-temperature-cofired-ceramics-based antenna in package, applied electromagnetics, and small antennas.

Roslina HUSSIN received the B.Sc. degree in Electrical Engineering from the University of Tulsa, United States of America in 1994, and the M.Sc. degree in Communication Engineering from Universiti Sains Malaysia (USM), Malaysia in 2016. She joined the School of Electrical and Electronic Engineering, USM as a Research Officer in 2011.

Zainal Arifin AHMAD received the B.S. degree in Materials Engineering from Universiti Sains Malaysia, Malaysia; the M.S. degree from the University of Manchester, Institute of Science and Technology, United Kingdom; and the Ph.D. degree from the University of Sheffield, United Kingdom. He is currently a Senior Professor with the School of Materials and Mineral Resources Engineering, Universiti Sains Malaysia, Malaysia. His current research interests include ZTA ceramic for cutting insert, low-temperature-cofired-ceramics-based circuits, metal-ceramic joining, crystal glaze ceramic, TCP bioceramic, and dielectric ceramic for antennas.

Mohamadariff OTHMAN received his Bachelor degree in Electronic Engineering from Multimedia University, Malaysia in 2006; the M.Sc. degree in RF and Microwave field from Universiti Sains Malaysia (USM), Malaysia in 2008; and the Ph.D. degree in Antenna and Propagation field from USM in 2015. He joined the Department of Electrical Engineering, University of Malaya, Malaysia as a Senior Lecturer in 2016 after serving a private university for almost one and half year. His research interests include 5G antenna, dielectric characterization, dielectric resonator antenna design, and optimization of antenna design.

Mohd Fariz Ab RAHMAN was born in Kota Bharu, Malaysia. He received the B.Eng. (Hons) degree in Materials Engineering from Universiti Malaysia Perlis, Malaysia in 2010; the M.Sc. and Ph.D. degrees in Materials Engineering from Universiti Sains Malaysia (USM), Malaysia in 2014 and 2017, respectively. In 2018, he joined the School of Electrical and Electronic Engineering, USM. He has authored more than 20 articles. His research interests include materials engineering, materials science and electroceramics which include the development of ceramic materials for electronic devices.